Oxygen-Isotope Effect on the In-Plane Penetration Depth in Underdoped $La_{2-x}Sr_xCuO_4$ Single Crystals

J. Hofer,[1] K. Conder,[2] T. Sasagawa,[3] Guo-meng Zhao,[1] M. Willemin,[1] H. Keller,[1] and K. Kishio[3]

[1]*Physik-Institut der Universität Zürich, Winterthurerstrasse 190, CH-8057 Zürich, Switzerland*

[2]*Laboratorium für Festkörperphysik, ETH Hönggerberg Zürich, CH-8093 Zürich, Switzerland*

[3]*Department of Superconductivity, University of Tokyo, 7-3-1 Hongo, Bunkyo-ku, Tokyo 113-8656, Japan*

(Received 20 December 1999)

We report measurements of the oxygen-isotope effect (OIE) on the in-plane penetration depth $\lambda_{ab}(0)$ in underdoped $La_{2-x}Sr_xCuO_4$ single crystals. A highly sensitive magnetic torque sensor with a resolution of $\Delta\tau \simeq 10^{-12}$ N m was used for the magnetic measurements on microcrystals with a mass of $\approx$10 μg. The OIE on $\lambda_{ab}^{-2}(0)$ is found to be $-10(2)\%$ for $x = 0.080$ and $-8(1)\%$ for $x = 0.086$. It arises mainly from the oxygen-mass dependence of the in-plane effective mass m_{ab}^*. The present results suggest that lattice vibrations are important for the occurrence of high temperature superconductivity.

PACS numbers: 74.25.Ha, 74.20.Mn, 82.20.Tr

Soon after the discovery of high temperature superconductivity [1] a large number of isotope-effect experiments were performed to investigate the pairing mechanism [2]. The very first oxygen-isotope studies were carried out on optimally doped samples and showed a negligible oxygen-isotope effect (OIE) [3]. A number of subsequent experiments revealed a dependence of T_c on the oxygen-isotope mass M_O [4–6] and on the copper-isotope mass M_{Cu} [7,8]. It was generally found that the isotope effects are large in the underdoped region but become small when the doping increases towards the optimally doped and overdoped regimes [5,8]. A large OIE on the Meissner fraction was observed in $La_{2-x}Sr_xCuO_4$ powder samples and attributed to a strong oxygen-mass dependence of the effective mass m^* of the superconducting charge carriers [9]. However, these experiments were made on powder samples and thus probed the average magnetic properties of this highly anisotropic superconductor. For a quantitative analysis, isotope experiments on single crystals are required.

Unfortunately, a complete oxygen-isotope exchange by diffusion is very difficult in single crystals with a large volume, as shown by a study on $Bi_2Sr_2CaCu_2O_{8+\delta}$ crystals with $V \approx 5 \times 4 \times 0.1$ mm^3 [10]. Indeed, our preliminary investigations on $La_{2-x}Sr_xCuO_4$ single crystals with $V \simeq 1 \times 1 \times 0.3$ mm^3 showed that a complete isotope exchange was not possible. In order to reach a complete oxygen-isotope exchange, microcrystals with a volume of only $V \approx 150 \times 150 \times 50$ μm^3 (mass $\approx$10 μg) were used for the present study. In these tiny samples, having a volume not very much larger than the grain size of polycrystalline samples, an almost complete oxygen-isotope exchange was achieved by diffusion, as shown below.

It is known that the transition temperature T_c and the in-plane penetration depth λ_{ab} of a cuprate superconductor can be determined from temperature- and field-dependent measurements of the reversible magnetization M using SQUID magnetometry [11]. Close to T_c the magnetic moment $m = VM$ of microcrystals with a mass of $\approx$10 μg lies well below the resolution $\Delta m = 10^{-10}$ A m^2 of commercial SQUID magnetometers. Therefore, all magnetic measurements were carried out using a highly sensitive torque magnetometer with a resolution $\Delta\tau < 10^{-12}$ N m [12]. The magnetic torque $\vec{\tau} = \vec{m} \times \vec{B}_a$ is usually recorded as a function of the angle δ between the field $\vec{B}_a$ and the c axis of the crystal [13,14]. However, when δ is fixed at a finite value, temperature- and field-dependent torque measurements can be performed as well. An appropriate angle to carry out these measurements is $\delta = 45°$ for the following reasons: (i) $\vec{m}$ is still pointing along the c axis due to the large anisotropy [15]. (ii) The magnetic torque $\tau = mB_a \sin(\delta)$ is sufficiently large to be measured for tiny magnetic moments in small fields. (iii) The reversible regime in the (B_a, T) phase diagram is almost as large as for $\delta = 0°$ [16], and a thermodynamic analysis of the measurements is possible over a wide temperature range. Thus, torque measurements performed at a fixed δ of 45° can be used to determine T_c from the temperature-dependent magnetization $M \propto \tau$, and to extract λ_{ab} from the field-dependent magnetization $M \propto \tau/B_a$.

Four microcrystals were cut from single crystals with Sr contents of $x = 0.080$ (samples Ia and Ib) and $x = 0.086$ (samples IIa and IIb), grown by the traveling-solvent-floating-zone method [17]. Underdoped samples were chosen for this study because the OIE is expected to be large in this doping regime [5]. For both sets of samples, I ($x = 0.080$) and II ($x = 0.086$), the oxygen-exchange procedure was as follows: Both samples a and b were annealed in ^{16}O in order to saturate the oxygen content. Then sample a was exchanged in an atmosphere with 97% ^{18}O while sample b was simultaneously treated in ^{16}O. Finally, sample a was backexchanged to ^{16}O while sample b was exchanged to ^{18}O. All exchange procedures were performed in 1 bar atmosphere at 950 °C for 50 h. The samples were cooled to room temperature with a cooling rate of 25 °C/h.

 0031-9007/00/84(18)/4192(4)$15.00

In order to measure the magnetic torque, the samples were mounted on a miniaturized cantilever with a piezoresistive readout and an integrated calibration loop [12]. The cantilever was placed between the poles of a conventional NMR magnet with a maximal field $B_a = 1.5$ T. The sensor was used in the so-called torsion mode [12], where major background effects arising from the strong temperature and field dependence of the piezoresistive paths were canceled out. In fact, the remaining temperature-dependent background of the cantilever was sufficiently small for performing temperature-dependent magnetic torque measurements.

The superconducting transition was studied by cooling the sample in a magnetic field $B_a = 0.1$ T applied at $\delta = 45°$. The torque signal was continuously recorded upon cooling the crystal at a cooling rate of 0.01 K/s. In order to determine the background signal of the cantilever, the measurement was repeated in zero field and the data were subtracted from those of the field-cooled measurement. The magnetic torque versus temperature obtained for the samples Ia and IIa is shown in Fig. 1. Clearly, T_c is lower for the ^{18}O exchanged samples. We define T_c as the temperature where the linearly extrapolated transition slope intersects the base line ($\tau = 0$ N m). The relative changes in T_c are found to be $\Delta T_c/T_c = [T_c(^{18}\mathrm{O}) - T_c(^{16}\mathrm{O})]/T_c(^{16}\mathrm{O}) = -5.5(4)\%$ for sample Ia and $\Delta T_c/T_c = -5.1(3)\%$ for sample IIa. The samples Ib and IIb showed no change in the superconducting transition after the second annealing in ^{16}O, which indicates a complete saturation of oxygen during the first annealing procedure. The oxygen-isotope shifts of T_c are summarized in Table I. As expected, they are larger for the samples Ia and Ib with a smaller x [5,18]. As shown in Fig. 1, the magnetic signals of the backexchanged samples (crosses) coincide with those of the ^{16}O annealed samples (open circles). This result implies that a complete backexchange from the ^{18}O to the ^{16}O isotope was achieved. This is only possible if after the backexchange procedure the ^{16}O enrichment in the sample corresponds to the ^{16}O concentration of the gas, which is 100% (the contamination of the ^{16}O atmosphere by the ^{18}O isotope removed from the crystal is less than 10 ppm and thus negligible). For the same reason, after exchanging ^{16}O with ^{18}O, the ^{18}O concentration of the sample is the same as that of the exchange atmosphere (i.e., 97% ^{18}O). The fact that the shift in T_c is parallel, with no broadening of the transition, also demonstrates an almost complete isotope exchange. The exponent α_{O} of the OIE on T_c is defined by $T_c \propto M_{\mathrm{O}}^{\alpha_{\mathrm{O}}}$. Taking into account a 97% exchange, we find $\alpha_{\mathrm{O}} = -(\Delta T_c/T_c)/(\Delta M_{\mathrm{O}}/M_{\mathrm{O}}) = 0.47(2)$ for $x = 0.080$ and $\alpha_{\mathrm{O}} = 0.40(2)$ for $x = 0.086$, which is in good agreement with the results obtained for powder samples with similar doping [5,18].

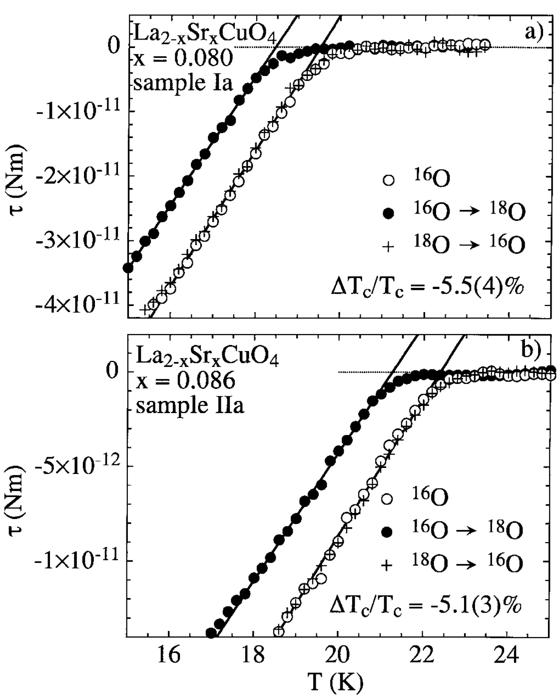

FIG. 1. Magnetic torque τ versus temperature, showing the OIE on T_c for samples Ia and IIa. The reproducibility of the exchange procedure, as checked by the backexchange (crosses), demonstrates a complete isotope exchange. For clarity not all measured data points are shown.

The in-plane penetration depth $\lambda_{ab}(T)$ was extracted from field-dependent measurements carried out at different temperatures with the field applied at $\delta = 45°$. At this angle a reversible signal was observed over a large field range down to 10 K. This allows the determination of $\lambda_{ab}(T)$ in a wide temperature range. The reversible part of the torque signal, $\tau/B_a \propto M$, recorded on sample Ib (after the second annealing in ^{16}O) at different temperatures is shown as a function of B_a in Fig. 2. The logarithmic field dependence, characteristic for an extreme type-II superconductor, is clearly seen for small applied fields. In this field regime the reversible torque is given by [13,19]

$$\frac{\tau}{B_a} = \frac{\alpha V \Phi_0}{8\pi^2 \mu_0 \lambda_{ab}^2(T)} \left(1 - \frac{1}{\gamma^2}\right) \frac{\sin 2\delta}{\epsilon(\delta)} \times \ln\left(\frac{\beta \xi_{ab}^2(T) \epsilon(\delta)}{\Phi_0} B_a\right), \quad (1)$$

where $\gamma = \sqrt{m_c^*/m_{ab}^*}$ is the effective mass anisotropy, $\xi_{ab}(T)$ is the in-plane correlation length, and $\epsilon(\delta) = (1/\gamma^2 \sin^2\delta + \cos^2\delta)^{1/2}$. The numerical factors α and β depend on the specific model [13,19]. Equation (1) is valid only for fields $B_a < B^*(T)$, where the data points in Fig. 2 lie on a straight line. As an example $B^*(T = 20.5\ \mathrm{K})$ is indicated by an arrow. For $B_a > B^*(T)$ the condition $B_a \ll \Phi_0/[\xi_{ab}^2(T)\epsilon(\delta)]$, for Eq. (1) to be valid [15,19], is no longer fulfilled.

For $\delta = 45°$ the dependence of τ/B_a in Eq. (1) on γ is very weak for large γ values, since $\epsilon(45°) \simeq \cos(45°)$. Nevertheless, a precise knowledge of γ is advantageous for extracting $\lambda_{ab}(T)$ from field-dependent measurements

TABLE I. Summary of the OIE results of the four $La_{2-x}Sr_xCuO_4$ single crystals with $x = 0.080$ (samples Ia and Ib) and $x = 0.086$ (samples IIa and IIb).

Sample	Mass [μg]	T_c (^{16}O) [K]	T_c (^{18}O) [K]	$\frac{\Delta T_c}{T_c}$ [%]	α_O	$\frac{\Delta\lambda_{ab}^{-2}(0)}{\lambda_{ab}^{-2}(0)}$ [%]
Ia	9.6	19.52(5)	18.45(5)	−5.5(4)	0.45(3)	−9(3)
Ib	12.1	19.68(5)	18.50(5)	−6.0(4)	0.49(3)	−11(3)
IIa	3.4	22.40(5)	21.26(5)	−5.1(3)	0.42(3)	−7(1)
IIb	3.8	22.11(5)	21.11(5)	−4.5(3)	0.37(3)	−10(1)
Mean I				−5.7(3)	0.47(2)	−10(2)
Mean II				−4.8(2)	0.40(2)	−8(1)

by use of Eq. (1). Therefore, in order to determine γ, angular-dependent torque measurements were performed close to T_c. Equation (1) can also be used to analyze angular-dependent torque data, provided that the measurements are performed at $B_a \leq B^*(T)$. In order to obtain a fully reversible signal over the whole angular regime in these small fields, we applied an additional ac field perpendicular to $\vec{B}_a$ in order to enhance the relaxation processes [20]. From these measurements γ was determined for each sample. The penetration depth $\lambda_{ab}^{-2}(T)$ was then extracted from the slope of the linear part of the field-dependent data (solid lines in Fig. 2), using Eq. (1) with γ fixed.

Figure 3 displays $\lambda_{ab}^{-2}(T)$ for the samples Ia and IIa. The temperature dependence is well described by the power law $\lambda_{ab}^{-2}(T) = \lambda_{ab}^{-2}(0)[1 - (T/T_c)^n]$ with an exponent $n \approx 5$. The fact that $\lambda_{ab}(T)$ can be determined down to $T \simeq 0.5T_c$ justifies the extrapolation of $\lambda_{ab}(T)$ to $T = 0$ K using this empirical power law. By normalizing the extracted $\lambda_{ab}^{-2}(T)$ values to the low temperature values $\lambda_{ab}^{-2}(0)$ obtained for the ^{18}O exchanged samples, any uncertainties in determining the sample volume V are avoided. From Fig. 3 it is evident that not only T_c but also $\lambda_{ab}^{-2}(0)$ shift upon replacing ^{16}O by ^{18}O. The shifts in T_c as obtained from the extrapolation are $\Delta T_c/T_c = -5.7(7)\%$ for sample Ia and $\Delta T_c/T_c = -3.7(7)\%$ for sample IIa. They are in good agreement with the T_c shifts found from the temperature-dependent measurements (see Table I). The shifts in $\lambda_{ab}^{-2}(0)$ are found to be $\Delta\lambda_{ab}^{-2}(0)/\lambda_{ab}^{-2}(0) = -9(3)\%$ and $-7(1)\%$ for the samples Ia ($x = 0.080$) and IIa ($x = 0.086$), respectively. Again, the data obtained on the backexchanged samples (crosses) coincide

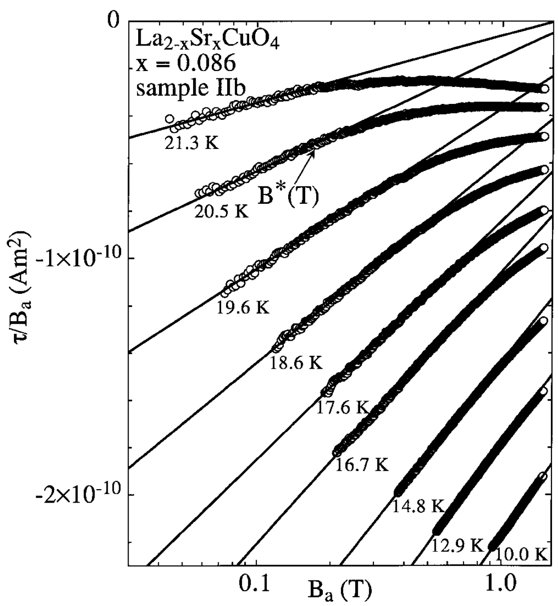

FIG. 2. Reversible part of the field-dependent torque $\tau/B_a \propto M$ versus B_a for sample IIb (after the second annealing in ^{16}O). The measurements were performed at different temperatures at fixed $\delta = 45°$. $\lambda_{ab}^{-2}(T)$ is extracted from the slope of the linear part of the data for $B_a \leq B^*(T)$ (solid lines) by using Eq. (1). For clarity some low temperature measurements are not shown.

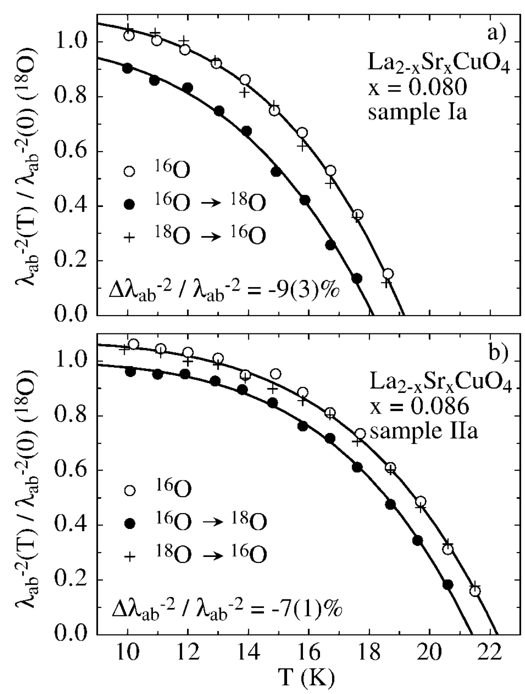

FIG. 3. Normalized in-plane penetration depth $\lambda_{ab}^{-2}(T)/\lambda_{ab}^{-2}(0)$ (^{18}O) for samples Ia and IIa. $\lambda_{ab}^{-2}(0)$ is determined by extrapolating the data to $T = 0$ K, using the power law $\lambda_{ab}^{-2}(T) = \lambda_{ab}^{-2}(0)[1 - (T/T_c)^n]$ (solid lines). The data of the backexchanged sample demonstrate the reproducibility of the exchange procedure.

with the data recorded after the first ^{16}O annealing. This demonstrates the reproducibility of the exchange procedure. A summary of the isotope effects obtained for all four samples is given in Table I.

Since $\lambda_{ab}^{-2}(0) \propto n_s/m_{ab}^*$, the oxygen-isotope shift of the penetration depth is due to a shift of n_s or m_{ab}^*,

$$\Delta\lambda_{ab}^{-2}(0)/\lambda_{ab}^{-2}(0) = \Delta n_s/n_s - \Delta m_{ab}^*/m_{ab}^* . \quad (2)$$

Several independent experiments on $La_{2-x}Sr_xCuO_4$ samples [9,18,21] have shown that the change of n_s during the exchange procedure is negligible. From this paper, further evidence that n_s is unchanged during the isotope exchange is given by the complete reproducibility of the exchange procedure. It is almost impossible that n_s changes upon ^{18}O substitution, but adopts again exactly the same value after the backexchange as in the ^{16}O annealed sample. We thus conclude that any change in n_s during the exchange procedure is negligible, and that the change of the in-plane penetration depth is mainly due to the isotope effect on the in-plane effective mass m_{ab}^*.

The observed OIE on m_{ab}^* gives strong evidence that lattice effects play an important role in high-T_c superconductivity. A possible explanation for the strong dependence of m_{ab}^* on the oxygen-isotope mass can be given by a model of small bipolarons, where $m_{ab}^* \propto m_{ab}\exp(g^2)$ (m_{ab} is the bare hole mass) [22]. Since the polaronic enhancement factor $g^2 \propto 1/\omega$ depends on the characteristic optical phonon frequency ω [22], a change of the frequency leads to a change of m_{ab}^*. The exponent of the total (copper and oxygen) isotope effect on m_{ab}^*, $\beta_{\rm tot} = \beta_{\rm Cu} + \beta_{\rm O}$, is then given by

$$\beta_{\rm tot} = -(\Delta m_{ab}^*/m_{ab}^*)/(\Delta M_{\rm r}/M_{\rm r}) = -0.5g^2. \quad (3)$$

The effective reduced mass $M_{\rm r}$ is a complicated function of $M_{\rm O}$ and $M_{\rm Cu}$, depending on the symmetry of the modes. From the experimentally observed shifts in $\lambda_{ab}^{-2}(0)$ we can determine the oxygen-isotope exponent $\beta_{\rm O} = -(\Delta m_{ab}^*/m_{ab}^*)/(\Delta M_{\rm O}/M_{\rm O})$. By taking a mean value of $\Delta\lambda_{ab}^{-2}(0)/\lambda_{ab}^{-2}(0) \simeq -9\%$ (see Table I) and using Eq. (2), we find $\beta_{\rm O} \simeq [\Delta\lambda_{ab}^{-2}(0)/\lambda_{ab}^{-2}(0)]/(\Delta M_{\rm O}/M_{\rm O}) \simeq -0.7$. A universal relation between T_c and $\lambda_{ab}^{-2}(0)$ was experimentally found in the cuprates, showing $T_c \propto \lambda_{ab}^{-2}(0)$ in the deeply underdoped regime [23]. If we consider a slightly weaker dependence of T_c on $\lambda_{ab}^{-2}(0)$ for the doping range investigated, we can assume $T_c \propto [\lambda_{ab}^{-2}(0)]^t$ with $t < 1$. We thus find $\alpha_{\rm O} \simeq -t\beta_{\rm O}$ (with $t \simeq 0.6$ from our experiment) and $\alpha_{\rm Cu} \simeq -t\beta_{\rm Cu}$. Since $\alpha_{\rm Cu}$ was found to be similar to $\alpha_{\rm O}$ [7,8], it is plausible to assume that $\beta_{\rm Cu} \simeq \beta_{\rm O}$ as well. We then find $\beta_{\rm tot} \simeq 2\beta_{\rm O} \simeq -1.4$ and thus $g^2 \simeq 2.8$ from Eq. (3). On the other hand, g^2 can also be determined from optical conductivity data, which according to the small polaron model show a maximum at $E_m = 2g^2\hbar\omega$ [22]. In $La_{2-x}Sr_xCuO_4$ this energy was found to be $E_m = 0.44$ eV for $x = 0.06$ and $E_m = 0.24$ eV for $x = 0.10$ [24]. For our samples with x lying between these two values, we expect $E_m \simeq 0.34$ eV. With $\hbar\omega \simeq 0.06$ eV [18] we thus find $g^2 \simeq 2.8$, in agreement with the magnitude of g^2 deduced from the OIE on m_{ab}^*.

In summary we have studied the OIE on T_c and on $\lambda_{ab}^{-2}(0)$ in underdoped $La_{2-x}Sr_xCuO_4$ microcrystals using a highly sensitive torque magnetometer. The reproducibility of the isotope-exchange procedure, as checked by backexchange, gives evidence for a complete isotope exchange in the single crystals. The isotope shift in $\lambda_{ab}^{-2}(0)$ is attributed to a shift in the in-plane effective mass m_{ab}^*. For $x = 0.080$ and $x = 0.086$ we find $\Delta m_{ab}^*/m_{ab}^* = -10(2)\%$ and $-8(1)\%$, respectively. The OIE on m_{ab}^* gives strong evidence that lattice vibrations play an important role in the occurrence of high temperature superconductivity.

We are grateful to A. Revcolevschi for providing the large single crystals on which the preliminary studies were performed. Fruitful discussions with C. Rossel are acknowledged. This work was partly supported by SNSF (Switzerland), NEDO, and CREST/JST (Japan). One of the authors (T. S.) would like to thank JSPS for financial support.

[1] J. G. Bednorz and K. A. Müller, Z. Phys. B **64**, 189 (1986).
[2] For a review, see J. P. Franck, in *Physical Properties of High Temperature Superconductors IV,* edited by D. M. Ginsberg (World Scientific, Singapore, 1994), pp. 189–293.
[3] B. Batlogg *et al.,* Phys. Rev. Lett. **58**, 2333 (1987).
[4] B. Batlogg *et al.,* Phys. Rev. Lett. **59**, 912 (1987).
[5] M. K. Crawford *et al.,* Phys. Rev. B **41**, 282 (1990).
[6] D. Zech *et al.,* Nature (London) **371**, 681 (1994).
[7] J. P. Franck, S. Harker, and J. H. Brewer, Phys. Rev. Lett. **71**, 283 (1993).
[8] G. M. Zhao *et al.,* Phys. Rev. B **54**, 14 956 (1996).
[9] G. M. Zhao *et al.,* Nature (London) **385**, 236 (1997).
[10] A. A. Martin and M. J. G. Lee, Physica (Amsterdam) **254C**, 222 (1995).
[11] Q. Li *et al.,* Phys. Rev. B **47**, 2854 (1993).
[12] M. Willemin *et al.,* J. Appl. Phys. **83**, 1163 (1998).
[13] D. E. Farrell *et al.,* Phys. Rev. Lett. **61**, 2805 (1988).
[14] J. Hofer *et al.,* Physica (Amsterdam) **297C**, 103 (1998).
[15] V. G. Kogan, M. M. Fang, and S. Mitra, Phys. Rev. B **38**, R11 958 (1988).
[16] G. Blatter *et al.,* Rev. Mod. Phys. **66**, 1125 (1994).
[17] T. Sasagawa *et al.,* Phys. Rev. Lett. **80**, 4297 (1998).
[18] G. M. Zhao *et al.,* J. Phys. Condens. Matter **10**, 9055 (1998).
[19] T. Schneider *et al.,* Eur. Phys. J. B **3**, 413 (1998); J. Hofer *et al.,* Phys. Rev. B **60**, 1332 (1999).
[20] M. Willemin *et al.,* Phys. Rev. B **58**, R5940 (1998).
[21] G. M. Zhao *et al.,* Phys. Rev. B **52**, 6840 (1995).
[22] A. S. Alexandrov and N. F. Mott, *Polarons and Bipolarons* (World Scientific, Singapore, 1995).
[23] T. Schneider and H. Keller, Int. J. Mod. Phys. **8**, 487 (1993).
[24] X. X. Bi and P. C. Eklund, Phys. Rev. Lett. **70**, 2625 (1993).